



## LETTER

# Protein-protein interaction analysis in crude bacterial lysates using combinational method of $^{19}\text{F}$ site-specific incorporation and $^{19}\text{F}$ NMR

Dear Editor,

Protein-protein interactions (PPI) are essential for a variety of cellular functions. Many PPI analyses were conducted *in vitro*, using purified proteins. In this report, the unnatural amino acid tfmF was site-specifically incorporated into several different sites of two Phox-Bem1 (PB1) domains from two mitogen activated protein kinases (MEKK3 and/ or MEK5) in the *E. coli* cells. Solution NMR  $^{19}\text{F}$  chemical shift and side chain relaxation analysis demonstrated that MEKK3-PB1-I57, MEKK3-PB1-F77, and MEK5-PB1-I70 sites were located in the interaction interface of the MEKK3/MEK5 complex, which was consistent with the crystal structure of MEKK3-PB1/MEK5-PB1 complex. Furthermore, crude lysates from *E. coli* cells with co-expressed tfmF incorporated MEKK3-PB1 and MEK5-PB1 were applied for  $^{19}\text{F}$  NMR analysis. The successful implementation of *in situ* PPI analysis using the combinational method of site-specific tfmF incorporation and  $^{19}\text{F}$  NMR demonstrated that this method could be a valuable general method for conformation and function studies of soluble multi-domain proteins or protein complexes in bacterial crude lysate, without procedures of protein purification.

Protein-protein interactions (PPI) play essential roles in cellular functions, such as DNA transcription, signal transduction, or cytoskeleton formation. Currently, a variety of techniques, including co-immunoprecipitation, isothermal titration calorimetry, and surface plasma resonance are frequently applied for PPI studies (Syafrizayanti et al., 2014). However, these methods can only provide the overall interaction pattern or internal motion of purified protein complexes, and have many limitations such as low specificity, high background or false positives (Syafrizayanti et al., 2014). Structure determination methods (such as X-ray crystallography and electron cryo-microscopy) can precisely illustrate protein interaction interface, while these structural methods require high concentration of purified proteins.

Recently, it has been reported that the cytoplasmic environment might have profound effects in regulating protein-protein and/or protein-ligand interactions that were hardly observed *in vitro* (Smith et al., 2014). The crucial

difference between *in vivo* and *in vitro* conditions lies in the high environmental concentration of diverse macromolecules, which is approximately 200 mg/mL in the eukaryotic cytoplasm and more than 400 mg/mL in prokaryotes (Mika and Poolman, 2011). Traditional *in vitro* biochemical studies of proteins were conducted in dilute solution with low macromolecular concentration (~10 mg/mL), which might not reveal protein-protein interaction or its mechanism in high fidelity.

Solution nuclear magnetic resonance (NMR) is powerful for PPI analysis and recently it has been applied to analyze protein conformation changes in living cells (Hansel et al., 2014). However, the traditional *in-cell* NMR method was hindered by low signal sensitivity and complicated resonance assignment of proteins *in vivo* (Hansel et al., 2014). At the same time, the solution NMR signals of large size proteins were very weak in intensity, with broad line width, due to slow global correlation time and rapid nuclei spin relaxation rate. Consequently, NMR resonance assignments of uniformly isotope labeled proteins will be very laborious due to strong overlaps in peaks with broad line width and low intensity. Alternatively, site-specific  $^{19}\text{F}$  incorporation and  $^{19}\text{F}$  NMR could provide a tool to implement PPI analysis *in situ* or *in vivo*. In the past decades,  $^{19}\text{F}$  NMR has been widely used for protein dynamic conformation changes and functional studies (Guo et al., 2015; Shi et al., 2011). Different from traditional multiple-site  $^{19}\text{F}$  incorporation through growing bacteria in media containing the  $^{19}\text{F}$ -aromatic residues (Lee et al., 2000), the  $^{19}\text{F}$ -containing unnatural amino acids could implement site-specific  $^{19}\text{F}$  labeling, resulting in the straightforward resonance assignment (Hammill et al., 2007; Li et al., 2010). The trifluoromethyl phenylalanine (tfmF) was successfully used for analyses of membrane protein's conformation changes, dynamics and functions (Shi et al., 2012). Additionally, the fast rotational motion of the  $\text{CF}_3$ -group in tfmF leads to a sharp single peak, which makes the tfmF- $^{19}\text{F}$  NMR method ideal for protein complex studies in high crowding conditions, such as cell lysate or cellular environment. Therefore, combinational application of the tfmF incorporation and  $^{19}\text{F}$  NMR for *in situ* PPI analysis would be immensely valuable, not only for PPI mechanism

studies, but also for PPI drug design with high specific and potent therapeutic principles against many diseases.

Here, the  $^{19}\text{F}$ -NMR PPI analysis in the native cellular environment was exemplified using the Phox and Bem1 (PB1) domains from two mitogen-activated protein kinases (MAPKs): MEKK3 and MEK5 (Drew et al., 2012). The MEKK3-PB1 domain (type II group) contains a positively charged basic cluster in the front end, whereas the MEK5-PB1 domain (type I group) contains a negatively charged acidic OPCA motif in the back end. The electrostatic interactions were known to be the major force for heterodimer formation between the type II MEKK3-PB1 and type I MEK5-PB1 in a front-to-back manner (Hu et al., 2007). In this report, the unnatural amino acid  $^{19}\text{F}$ -tfmF was incorporated into several sites of MEKK3-PB1 and MEK5-PB1, respectively. Then,  $^{19}\text{F}$  NMR chemical shift and relaxation data were obtained to analyze the interaction interfaces between MEKK3-PB1 and MEK5-PB1. The  $^{19}\text{F}$  chemical shift perturbations of residues in the interfacial region of MEKK3-PB1/MEK5-PB1 complex in crude bacterial cell lysates (without protein purification) were observed to be consistent not only with the  $^{19}\text{F}$  chemical shift data of the purified protein complex, but also with the crystal structure of the MEKK3-PB1/MEK5-PB1 complex, which strongly indicated the validity of the proposed general method of  $^{19}\text{F}$ -tfmF/ $^{19}\text{F}$ -NMR for *in situ* PPI analysis.

As shown in Fig. 1A, four residue sites (MEKK3-I57, MEKK3-F77, MEK5-I70 and MEK5-F41) were selected for site-specific tfmF incorporations. Size-exclusion chromatography (SEC) was applied to verify the complex formation between MEKK3-PB1-I57tfmF and MEK5-PB1-I70tfmF. In the SEC diagram, the earlier retention time of the MEKK3-PB1-tfmF/MEK5-PB1-tfmF than the MEKK3-PB1 or MEK5-PB1 indicated the stable complex formation (Fig. 1B). Single band in SDS-PAGE of purified MEKK3-PB1-I57tfmF and/or MEK5-PB1-I70tfmF with  $\text{Ni}^{2+}$ -NTA affinity chromatography demonstrated a good purity of these proteins (Fig. 1B, inset). MEKK3-PB1 and MEK5-PB1 were co-expressed using plasmid pETDuet-1 for site-specific tfmF-incorporation, and were co-purified using  $\text{Ni}^{2+}$ -NTA affinity chromatography (Fig. 1B, lane 1). Minor migration difference between the two bands was observed for  $^{19}\text{F}$ -MEK5-PB1 (lane 2) or  $^{19}\text{F}$ -MEKK3-PB1 (lane 3) (Fig. 1B).

To reveal motional properties of the tfmF-incorporation site and details of protein-protein interactions, both  $^{19}\text{F}$  longitudinal ( $T_1$ ) and transverse ( $T_2$ ) relaxation values of proteins with incorporated  $^{19}\text{F}$ -tfmF were measured. Here, the  $^{19}\text{F}$   $T_1$  and  $T_2$  relaxation values of MEKK3-PB1-F77tfmF in the absence or presence of wild-type MEK5-PB1 were shown as Fig. 1C–F. Upon addition of MEK5-PB1, the  $T_1$  relaxation value of MEK5-PB1-F77tfmF was observed to increase (Fig. 1C and 1E), whereas the  $T_2$  relaxation value decreased (Fig. 1D and 1F). The  $^{19}\text{F}$  relaxation values of the four tfmF incorporation sites (MEKK3-PB1-F77tfmF/MEK5-PB1, MEKK3-PB1-I57tfmF/MEK5-PB1, MEKK3-PB1-I70tfmF, MEKK3-PB1/MEK5-PB1-F41tfmF) were shown in

both Fig. 1 and Table S1 (supporting information). The pronounced decrease in  $T_2$  values in the presence of another domain could be attributed to the decreased global motion with increased molecular size or restrained internal motions (Palmer, 1993). Considering the halved global correlation time for the formation of MEKK3-PB1/MEK5-PB1 complex (the almost doubled molecular weight), the decreased relaxation data demonstrated the formation of a stable complex between MEKK3-PB1 and MEK5-PB1.

To investigate the PPI interface between MEKK3-PB1 and MEK5-PB1, *in vitro*  $^{19}\text{F}$  chemical shift of MEKK3-PB1-I57tfmF and MEKK3-PB1-F77tfmF were acquired in the absence or presence of the wild-type MEK5-PB1. Similarly, the  $^{19}\text{F}$  chemical shift of MEK5-PB1-I70tfmF and MEK5-PB1-F41tfmF were collected in the absence or presence of the wild-type MEKK3-PB1. Pronounced  $^{19}\text{F}$  chemical shift changes in the absence and presence of wild-type MEK5-PB1 (or MEKK3-PB1) were observed for MEKK3-PB1-I57tfmF, MEK5-PB1-I70tfmF and MEKK3-PB1-F77tfmF (Fig. 1G, 1K, 1H, 1L, 1I and 1M). The tertiary structure of the MEKK3-PB1 (PDB Number: 2C60), MEK5-PB1 and MEKK3-PB1/MEK5-PB1 complex (PDB Number: 2O2V) in PDB did not show pronounced structure variations in these sites after complex formation. The observations of chemical shift changes indicated that the sites I57 and F77 of MEKK3-PB1 and I70 of MEK5-PB1 were located in the interaction interface of the MEKK3-PB1/MEK5-PB1 complex. However, no obvious chemical shift changes were observed for MEK5-F41tfmF (Fig. 1J and 1N), which might be away from the PPI interface (the chemical shift values of  $^{19}\text{F}$  site-specific-labeled residues were presented in Table S1). The observations of chemical shift changes upon protein interaction were consistent with the three-dimensional crystal structure of the MEKK3-PB1 and MEK5-PB1 complex (PDB 2O2V).

To implement the *in situ* PPI analysis, the combinational method of tfmF-incorporation and  $^{19}\text{F}$ -NMR was also applied. In physiological cytosolic conditions, proteins are known to stay in a highly crowded environment with vast of non-specific interactions. Therefore, the conventional *in vitro* protein-protein interaction mode might not represent the real situation in the physiological environment. Because the cell lysate composed of mixture of soluble biomolecules in the host cells, the PPI analysis in cell lysates could contain the vast varieties of proteins in the crowded environment, avoiding perturbations of PPI during the protein purification procedures. To implement the PPI analysis between MEKK3-PB1 and MEK5-PB1 in crude lysates, the two proteins were co-expressed in *E. coli* and the crude cell lysates were prepared as shown in Fig. 2A. Due to the pronounced chemical shift changes in purified MEKK3-PB1-I57tfmF and purified MEK5-PB1-I70tfmF, these two sites were selected for double site-specific labeling. One-dimension  $^{19}\text{F}$  spectra of the purified sample or crude lysate sample containing MEKK3-PB1-I57tfmF are shown in Fig. 2B and E. Only one  $^{19}\text{F}$  peak was observed for both the purified MEKK3-PB1-

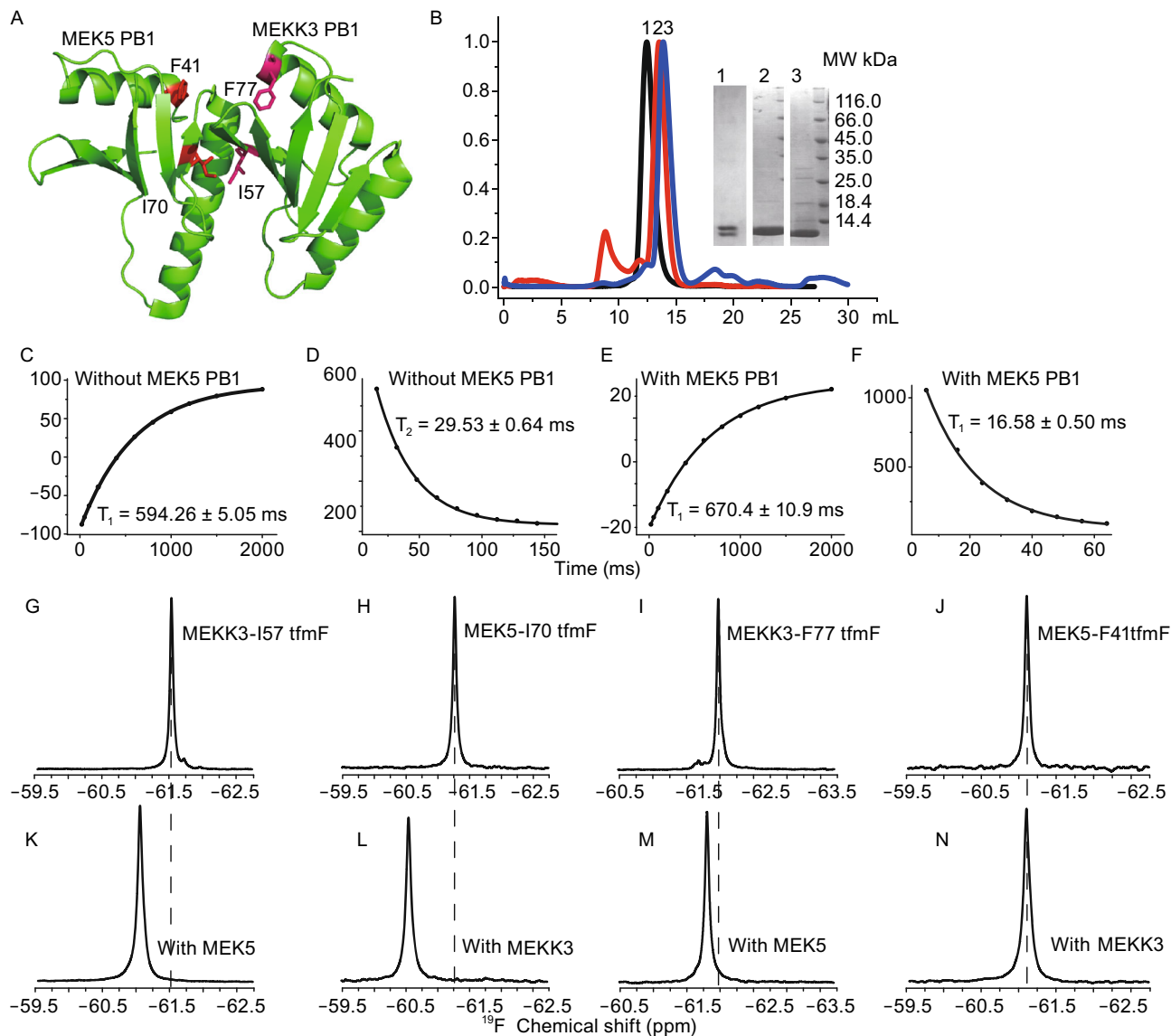


**Figure 1.**  $^{19}\text{F}$  chemical shift perturbations and relaxation values of site-specific *tfmF* incorporation in purified MEKK3-PB1 or MEK5-PB1. (A) Stereo ribbon drawing of the tertiary structure of the MEKK3-PB1 and MEK5-PB1 complex (PDB Number: 2O2V). The site-specific  $^{19}\text{F}$  incorporation sites (MEKK3-I57, MEKK3-F77, MEK5-I70, MEK5-F41) were coloured magenta and cyan in MEKK3-PB1 and MEK5-PB1 respectively. The figure was prepared using pymol. (B) Size exclusive chromatography of MEKK3-PB1 (blue), MEK5-PB1 (red), MEKK3-PB1/MEK5-PB1 complex (black) with *tfmF* incorporations. SDS-PAGE of MEKK3-PB1 (lane 3), MEK5-PB1 (lane 2), and co-purified MEKK3-PB1/MEK5-PB1, all with  $^{19}\text{F}$  incorporation (lane 1). Side chain longitudinal  $T_1$  (C and E) and transverse  $T_2$  (D and F) relaxation analysis of  $^{19}\text{F}$  site-specifically incorporated at the F77 site of MEKK3, in the absence or presence of MEK5-PB1 domain. One-dimension  $^{19}\text{F}$  spectra of *tfmF* incorporated MEKK3-PB1 domain in the absence (G and I) or presence (K and M) of the MEK5-PB1 domain. One-dimension  $^{19}\text{F}$  spectra of *tfmF* incorporated MEK5-PB1 domain in the absence (H and J) or presence (L and N) of the MEKK3-PB1 domain.

I57*tfmF* and the crude lysate sample, whereas the line width of the  $^{19}\text{F}$ -signal from the crude lysate sample was broader, obviously due to the crowding cellular environment, presence of non-specific protein interactions or chemical transient interactions in the crude lysate (Smith et al., 2014;

Latham and Kay, 2013). The  $^{19}\text{F}$  NMR spectra of MEK5-PB1-I70*tfmF* in the purification buffer and crude lysate are shown in Fig. 2C and F, with an increased line-width for MEK5-PB1-I70*tfmF* in the crude lysate. For the samples of two *tfmF*-incorporated proteins, two peaks were observed for

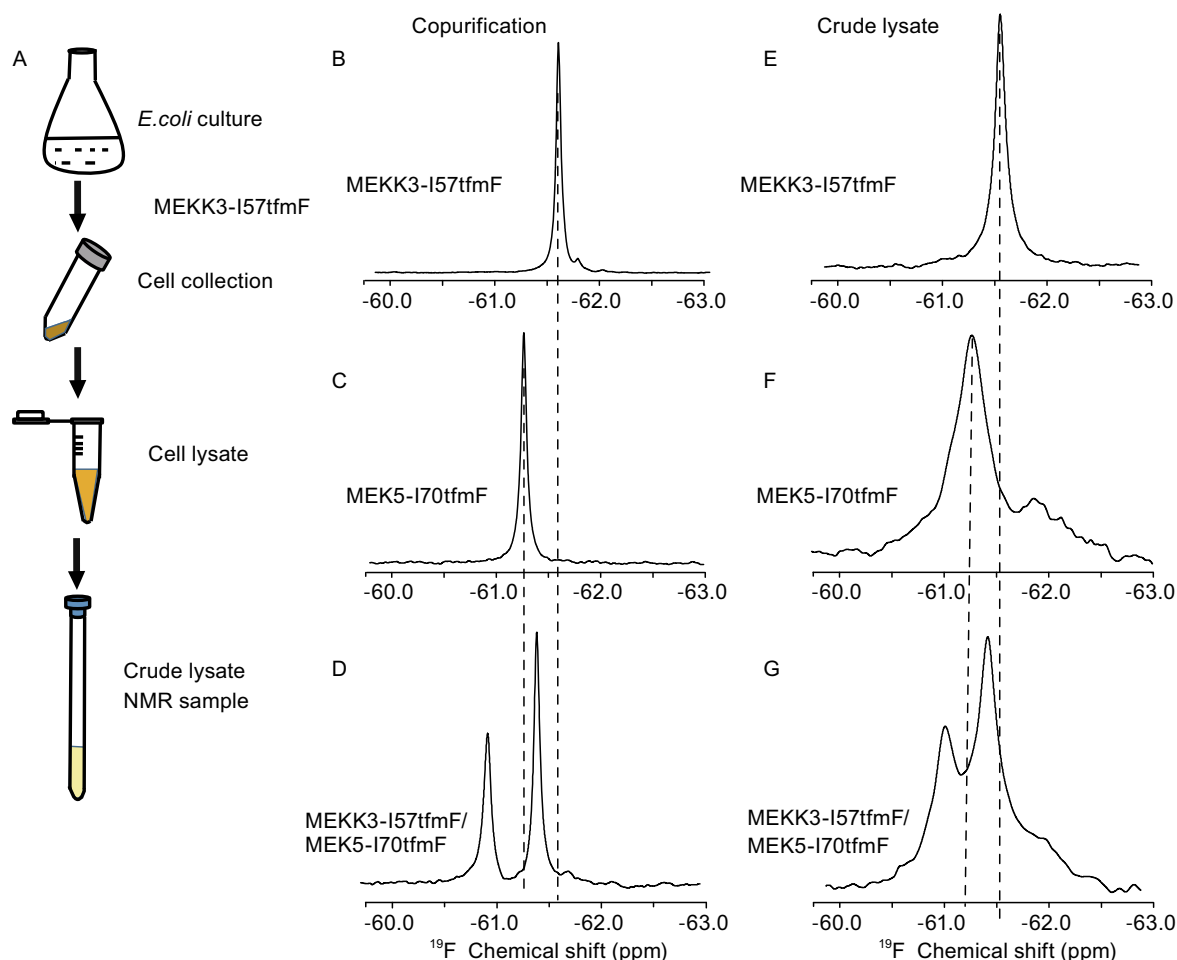


**Figure 2. One dimensional  $^{19}\text{F}$  NMR spectra of MEKK3-PB1 or MEK5-PB1 in crude lysates with double site-specific tfmF incorporation.** Procedure of crude lysate sample preparation (A), One-dimension  $^{19}\text{F}$  spectra of purified MEKK3-PB1-I57tfmF (B), MEK5-PB1-I70tfmF (C), and co-expressed MEKK3-PB1-I57tfmF and MEK5-PB1-I70tfmF complex (D). One-dimension  $^{19}\text{F}$  spectra of MEKK3-PB1-I57tfmF (E), MEK5-PB1-I70tfmF (F), and co-expressed MEKK3-PB1-I57tfmF and MEK5-PB1-I70tfmF complex in bacteria crude lysate (G).

the co-purified sample of MEKK3-PB1-I57tfmF and MEK5-PB1-I70tfmF. As shown in Fig. 1G, K, H, and L, the  $^{19}\text{F}$  chemical shifts of MEKK3-PB1-I57tfmF and MEK5-PB1-I70tfmF were shifted downfield upon protein interaction. According to the  $^{19}\text{F}$  chemical shift values (Table S1) with single site labeling, the right peak in Fig. 2D could be assigned to MEKK3-PB1-I57tfmF, whereas the left was assigned to MEK5-PB1-I70tfmF. A significant shift of the  $^{19}\text{F}$  signal of MEKK3-PB1-I57tfmF and MEK5-PB1-I70tfmF were observed upon the presence of partner proteins of the complex, or in the presence of specific protein-protein interactions.

Additionally, different from  $^{19}\text{F}$  signals of the co-purified sample, two wider  $^{19}\text{F}$  signals were shown in Fig. 2G as a result of co-expressed proteins in crude lysate samples. The  $^{19}\text{F}$  NMR signals from crude lysates were much broader, due

to molecular crowding or weak transient interactions in the crude lysate (Smith et al., 2014; Latham and Kay, 2013). Compared with solution NMR data of purified co-expression MEKK3-PB1 and MEK5-PB1, the crude lysate data illustrated that  $^{19}\text{F}$  chemical shift values of residues in crude lysate were influenced by the ubiquitous nature of weak, non-specific interactions in cells, which retarded the rotational motion of soluble proteins and the exchange dynamics. The increased line width of 1D  $^{19}\text{F}$  NMR spectra in the crude lysate sample presented the physiological environment of cell plasma.

Referring to the observed chemical shift perturbations of MEKK3-PB1-I57tfmF/ MEK5-PB1-I70tfmF in the *in vitro* PPI studies (Figs. 1G–N and 2B–D), the observed  $^{19}\text{F}$  chemical shift perturbations of the *in situ* PPI studies (Fig. 2E–G) verified the existence of protein interactions between

MEKK3-PB1 and MEK5-PB1 in the *E. coli* cytosols, even in the presence of extensive, non-specific macromolecular interactions in cell lysate. For the MEKK3-PB1/MEK5-PB1 protein complex, the physicochemical mechanisms governing macromolecular assembly in the cell must be similar as those in cell extracts (Luh et al., 2013). At the same time, the increased line widths of  $^{19}\text{F}$  NMR signals of proteins in crude lysate implied the availability of many non-specific interactions with the target proteins, through some universal mechanisms like hydrogen bonds, charge-charge interactions, or random collisions in the cellular environment.

Normally, more than one condition could lead to the  $^{19}\text{F}$  chemical shift changes of the tfmF incorporation site: the localization in the PPI interface, or allosteric conformational changes after protein-protein interaction. Nevertheless, the  $^{19}\text{F}$ -tfmF chemical shifts could represent the availability of protein-protein interactions, in cell lysate or other in-cell mimic conditions. Of course, multiple site incorporations of tfmF and  $^{19}\text{F}$ -NMR will be required to reflect the uniform changes of the sample conditions, e.g. acidification, viscosity changes or protein degradation. In this report the  $^{19}\text{F}$ -spectra of MEK5-F41tfmF (Fig. 1J and 1N) were working as the control to reflect the macro-scale condition changes.

To distinguish the PPI interface or the allosteric conformation changes, further  $^{19}\text{F}$ -detected relaxation analysis should be conducted. For the residue sites in the PPI interface, not only the  $^{19}\text{F}$  chemical shift changes were expected, but also variations of the  $T_1$  relaxation (spin-lattice),  $T_2$  relaxation (spin-spin diffusion) could be observed. However, for the allosteric conformation changes, the conformational exchange ( $\tau_{\text{ex}}$ ) and  $T_2$  relaxation exchanges could be observed.

In summary, combinational method of site-specifically incorporation of the unnatural amino acid tfmF into proteins and  $^{19}\text{F}$  NMR could be a reliable method for PPI analysis in cellular cytosols, taking advantage of no natural  $^{19}\text{F}$  background signals from cellular molecules. At the same time, the tfmF incorporations at two residue sites using the pET-Duet plasmids in this report provided a general method for *in situ* PPI analysis between two tfmF-incorporated proteins. Therefore, conformational and functional studies of other soluble proteins (enzymes, receptors), or interaction interfaces analysis of two proteins in a complex in crude cell lysates could be implemented using the combinational method of site-specific  $^{19}\text{F}$  incorporation and  $^{19}\text{F}$  NMR.



## FOOTNOTES

Authors are grateful for kind courtesy of plasmid pDule-tfmF from Dr. R. A. Mehl, Department of Biochemistry and Biophysics, Oregon State University, 2011 Agriculture and Life Sciences Building, Corvallis, Oregon 97331, United States.

This work was supported by the Chinese Key Research Plan—Protein Science (2013CB910200, 2015CB910100), and National

Natural Science Foundation of China (Grant Nos. U1332138, U1432136, U1332210 and 31300685).

Dong Li, Yanan Zhang, Yao He, Chengwei Zhang, Jiefei Wang, Ying Xiong, Longhua Zhang, Yangzhong Liu, Pan Shi, and Changlin Tian declare that they have no conflict of interest. This article does not contain any studies with human or animal subjects performed by the any of the authors.

Dong Li<sup>1</sup>, Yanan Zhang<sup>1</sup>, Yao He<sup>1</sup>, Chengwei Zhang<sup>1</sup>, Jiefei Wang<sup>1</sup>, Ying Xiong<sup>1</sup>, Longhua Zhang<sup>1</sup>, Yangzhong Liu<sup>2</sup>, Pan Shi<sup>1</sup> , Changlin Tian<sup>1</sup> 

<sup>1</sup> Hefei National Laboratory for Physical Science at the Microscale School of Life Science, University of Science and Technology of China, Hefei 230026, Anhui, China

<sup>2</sup> School of Chemistry, University of Science and Technology of China, Hefei 230026, Anhui, China

## OPEN ACCESS

This article is distributed under the terms of the Creative Commons Attribution 4.0 International License (<http://creativecommons.org/licenses/by/4.0/>), which permits unrestricted use, distribution, and reproduction in any medium, provided you give appropriate credit to the original author(s) and the source, provide a link to the Creative Commons license, and indicate if changes were made.

## REFERENCES

- Drew BA, Burow ME, Beckman BS (2012) MEK5/ERK5 pathway: the first fifteen years. *Biochim Biophys Acta* 1825:37–48
- Guo X, Wang L, Li J, Ding Z, Xiao J et al (2015) Structural insight into autoinhibition and histone H3-induced activation of DNMT3A. *Nature* 517:640–644
- Hammill JT, Miyake-Stoner S, Hazen JL, Jackson JC, Mehl RA (2007) Preparation of site-specifically labeled fluorinated proteins for  $^{19}\text{F}$ -NMR structural characterization. *Nat Protoc* 2:2601–2607
- Hansel R, Luh LM, Corbeski I, Trantirek L, Dotsch V (2014) In-cell NMR and EPR spectroscopy of biomacromolecules. *Angew Chem Int Ed Engl* 53:10300–10314
- Hu Q, Shen W, Huang H, Liu J, Zhang J et al (2007) Insight into the binding properties of MEKK3 PB1 to MEK5 PB1 from its solution structure. *Biochemistry* 46:13478–13489
- Latham MP, Kay LE (2013) Probing non-specific interactions of Ca(2+)-calmodulin in *E. coli* lysate. *J Biomol NMR* 55:239–247
- Lee HW, Sohn JH, Yeh BI, Choi JW, Jung S et al (2000)  $^{19}\text{F}$  NMR investigation of F(1)-ATPase of *Escherichia coli* using fluorotryptophan labeling. *J Biochem* 127:1053–1056
- Li C, Wang GF, Wang Y, Creager-Allen R, Lutz EA et al (2010) Protein ( $^{19}\text{F}$ ) NMR in *Escherichia coli*. *J Am Chem Soc* 132:321–327
- Luh LM, Hansel R, Lohr F, Kirchner DK, Krauskopf K et al (2013) Molecular crowding drives active Pin1 into nonspecific

- complexes with endogenous proteins prior to substrate recognition. *J Am Chem Soc* 135:13796–13803
- Mika JT, Poolman B (2011) Macromolecule diffusion and confinement in prokaryotic cells. *Curr Opin Biotechnol* 22:117–126
- Palmer AG 3rd (1993) Dynamic properties of proteins from NMR spectroscopy. *Curr Opin Biotechnol* 4:385–391
- Shi P, Wang H, Xi Z, Shi C, Xiong Y et al (2011) Site-specific (1)(9)F NMR chemical shift and side chain relaxation analysis of a membrane protein labeled with an unnatural amino acid. *Protein Sci* 20:224–228
- Shi P, Li D, Chen H, Xiong Y, Wang Y et al (2012) In situ 19F NMR studies of an *E. coli* membrane protein. *Protein Sci* 21:596–600
- Smith AE, Zhang Z, Pielak GJ, Li C (2014) NMR studies of protein folding and binding in cells and cell-like environments. *Curr Opin Struct Biol* 30C:7–16
- Syafrizayanti Betzen C, Hoheisel JD, Kastelic D (2014) Methods for analyzing and quantifying protein-protein interaction. *Expert Rev Proteomics* 11:107–120

---

Dong Li and Yanan Zhang have contributed equally to this work.

**Electronic supplementary material** The online version of this article (doi:[10.1007/s13238-016-0336-8](https://doi.org/10.1007/s13238-016-0336-8)) contains supplementary material, which is available to authorized users.